ELSEVIER

Journal of Alloys and Compounds 388 (2005) 303–307

Journal of ALLOYS AND COMPOUNDS

www.elsevier.com/locate/jallcom

Effect of Zr additions on the electrode characteristics of nanocrystalline TiNi-type hydrogen storage alloys

M. Makowiecka[a], E. Jankowska[b], I. Okonska[a], M. Jurczyk[a,*]

[a] *Institute of Materials Science and Engineering, Poznan University of Technology, M. Sklodowska Curie 5 Sq., 60-965 Poznan, Poland*

[b] *Central Laboratory of Batteries and Cells, Forteczna 12/14 St., 61-362 Poznan, Poland*

Received 4 July 2004; received in revised form 26 July 2004; accepted 28 July 2004

Abstract

The effect of Zr on the structure and electrochemical properties of nanocrystalline TiNi-type alloys was studied. These materials were prepared by mechanical alloying (MA) followed by annealing. It was found that the respective replacement of Ni in nanocrystalline TiNi by Zr, and by Zr and Fe improved not only the discharge capacity but also the cycle life of these electrodes. In the nanocrystalline $TiNi_{0.875}Zr_{0.125}$, a powder discharge capacity up to 135 mA h g^{-1} was measured on the 10th cycle (at 40 mA g^{-1} discharge current). The studies show that the electrochemical properties of Ni-MH batteries are a function of the microstructure and the chemical composition of the used electrode materials.

© 2004 Elsevier B.V. All rights reserved.

Keywords: Alloys; Nanostructures; Electrochemical properties

1. Introduction

Recently, mechanical alloying (MA) has been used to produce nanocrystalline TiFe, $LaNi_5$, ZrV_2 and Mg_2Ni-type alloys [1–6]. MA is a solid state powder processing technique, which involves repeated welding, fracturing and rewelding of powder particles in a high-energy ball mill [7,8]. The nanostructured materials show substantially enhanced absorption and desorption kinetics, even at relatively low temperatures [2].

Among the different types of hydride-forming compounds, TiNi-type alloys are among the most promising electrode materials for nickel-metal hydride (Ni-MH) batteries. The polycrystalline TiNi system has been widely studied in the past [9–13]. TiNi alloy, which crystallizes in the cubic CsCl-type structure, is lighter and cheaper than the $LaNi_5$-type material and can absorb up to 1 H/f.u. at room temperature. A discharge capacity larger than 200 mA h g^{-1} was reported for polycrystalline TiNi (at 5 mA g^{-1} discharge current) [13].

To improve the activation of this alloy, several approaches have been adopted. Increasing the Ni content [14], substituting Nb and Pd [13] and B [15] for nickel and Ni or Cu micro-encapsulation all enhance markedly the cycle life of TiNi electrodes. On the other hand, high-energy ball-milling (HEBM) is effective for the improvement of the initial hydrogen absorption rate, due to the reduction in the particle size and the creation of new clean surfaces [16]. The production by mechanically alloyed $TiFe_{1-x}Ni_x$ ($0 \leq x \leq 1$) alloys has been published [3,4]. Materials obtained by the substitution of Ni for Fe in $TiFe_{1-x}Ni_x$ led to great improvement in activation behaviour of the electrodes. It was found that the increasing nickel content in $TiFe_{1-x}Ni_x$ alloys leads initially to an increase in discharge capacity, giving a maximum at $x = 0.75$. In the annealed nanocrystalline $TiFe_{0.25}Ni_{0.75}$ powder, a discharge capacity of up to 155 mA h g^{-1} was measured (at 40 mA g^{-1} discharge current). The electrodes made from mechanically alloyed and annealed elemental powders displayed maximum capacities at around the third cycle, but especially

* Corresponding author. Tel.: +48 61 665 3508; fax: +48 61 665 3576.
E-mail address: jurczyk@sol.put.poznan.pl (M. Jurczyk).

0925-8388/$ – see front matter © 2004 Elsevier B.V. All rights reserved.
doi:10.1016/j.jallcom.2004.07.026

for x = 0.5 and 0.75 in $TiFe_{1-x}Ni_x$ alloy, degraded slightly with cycling. Generally, it was accepted that the oxidation and segregation of titanium were prominent factors associated with the capacity loss during charge–discharge cycling [13].

As shown earlier, nanocrystalline powders have a larger capacity than the amorphous parent alloy materials [2,3,6]. Annealing leads to grain growth, release of microstrain and to an increase of the storage capacity [2]. This behaviour is due to a well-established diffusion path for hydrogen atoms along the numerous grain boundaries [1].

In this work, we have prepared nanocrystalline TiNi-type hydrogen storage alloys. The 3d alloying elements Zr, or Zr and Fe, were substituted for nickel in TiNi, and the structural and electrochemical properties were studied.

2. Experimental

MA was performed under argon atmosphere using a SPEX 8000 Mixer Mill. The purity of the starting materials was at least 99.8% and the composition of the starting powder mixture corresponded to the stoichiometry of the "ideal" reactions. In the case of $LaNi_5$-type alloys, an extra 8 wt.% of rare earth was used. The elemental powders (Ti: ≤45 μm, Fe: 10 μm, Ni: 3−7 μm, Zr: ≤150 μm) were mixed and poured into the vial. The mill was run up to 20 h for every powder preparation. The as-milled powders were heat-treated at 700 °C for 0.5 h under high-purity argon to form ordered phases. The powders were characterized by means of X-ray diffraction (XRD) and atomic force microscopy (AFM). XRD were performed using a X-ray powder diffractometer with Co Kα radiation, at the various stages during milling, prior to annealing and after annealing.

The mechanically alloyed materials in nanocrystalline forms, with 10 wt.% addition of Ni powder, were subjected to electrochemical measurements as working electrodes. A detailed description of the electrochemical measurements was given in refs. [4,16].

3. Results and discussion

The effect of MA processing was studied by X-ray diffraction, microstructural investigations, AFM as well as by electrochemical measurements. In the present study, TiNi-type alloys have been prepared by MA followed by annealing (see text for details). During MA, the originally sharp diffraction

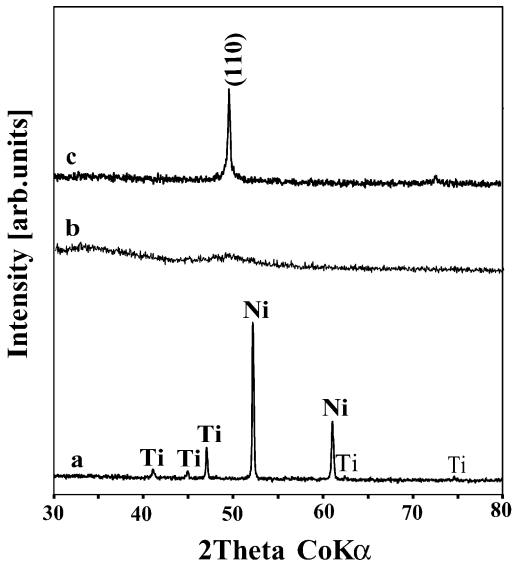

Fig. 1. XRD spectra of a mixture of Ti and Ni powders mechanically alloyed for different times: (a) 0 h, (b) 5 h and (c) after annealing at 700 °C/0.5 h.

lines of Ti and Ni gradually become broader, and their intensity decreases with milling time (Fig. 1). The powder mixture milled for more than 5 h has transformed completely to an amorphous phase, without the formation of another phase. But differentiation between a "truly" amorphous material, an extremely fine-grained material or a material in which very small crystals are embedded in an amorphous matrix has not been easy on the basis of the diffraction data. Only a supplementary investigation by neutron diffraction unambiguously confirmed that the phases produced by MA are truly amorphous [8]. The milled powder is finally heat-treated to obtain the desired microstructure and properties. Formation of the nanocrystalline alloys was achieved by annealing of the amorphous material in high-purity argon atmosphere at 700 °C for 0.5 h. The diffraction peaks were assigned to those of CsCl-type structure with a cell parameter a = 3.018 Å (Fig. 1c; Table 1).

The SEM technique was used to follow the changes in size and shape of the mechanically alloyed powder mixtures as a function of milling time (Fig. 2). The microstructure that forms during MA consists of layers of the starting material. The lamellar structure is increasingly refined during further MA. The thickness of the material decreases with the increase in MA time leading to true alloy formation. The sample shows cleavage fracture morphology and inhomogeneous size distribution. Many small powder particles have a tendency to agglomerate. The average crystallite size of the

Table 1
Lattice constants before and after hydrogenation and discharge capacities on 15th cycle for TiNi-type alloys produced by MA and annealing (700 °C/0.5 h)

Lattice constants	TiNi	$TiNi_{0.875}Zr_{0.125}$	$TiNi_{0.75}Fe_{0.25}$	$TiNi_{0.75}Fe_{0.125}Zr_{0.125}$
a (Å)	3.018	3.029	3.010	3.024
a_H (Å)	3.142	3.156	3.130	3.149
Discharge capacity on 15th cycle (mA h g^{-1})	79	134	90	128

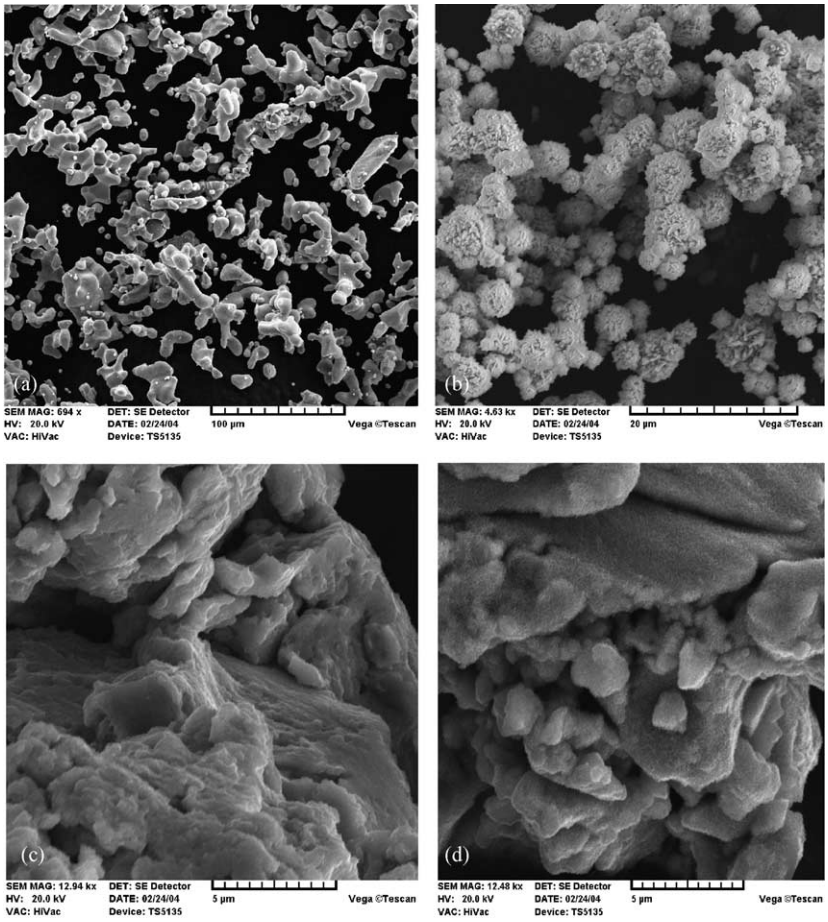

Fig. 2. SEM of powders: (a) Ti, (b) Ni, (c) after 5 h of MA and (d) after annealing at 700 °C/0.5 h.

nanocrystalline TiNi powders, according to AFM studies, was of the order of 25 nm (Fig. 3).

The electrochemical pressure-composition (e.p.c.) isotherms for absorption and desorption for the alloy electrode tested were determined by measurements of the equilibruim potential during intermittent electrode charge and discharge cycles at constant current density. The equilibruim hydrogen pressures were calculated using the Nerst equation. The e.p.c. isotherms determined on the amorphous and nanocrystalline TiNi alloys are illustrated in Fig. 4. The isotherms show an increase of the equilibrium hydrogen pressure and a decrease in the amount of hydrogen absorbed for the amorphous alloy (curve a) in comparison with the nanocrystalline alloy (curve b).

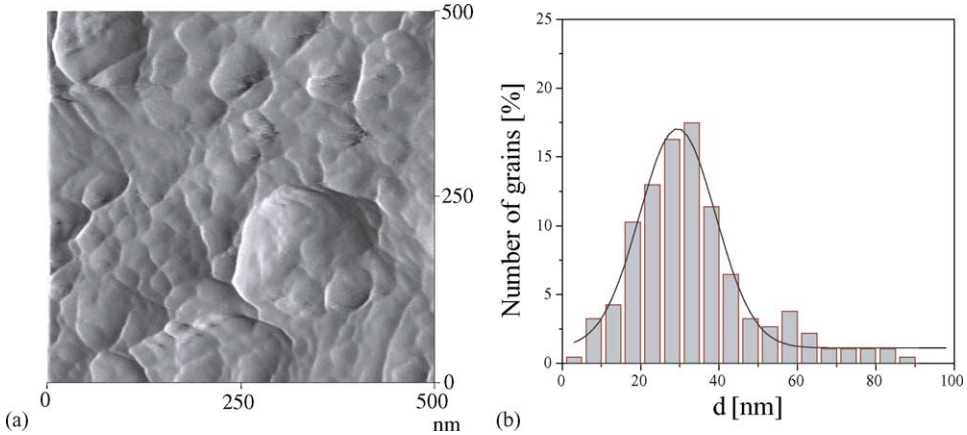

Fig. 3. AFM photograph of nanocrystalline TiNi alloy (a) and histogram (b).

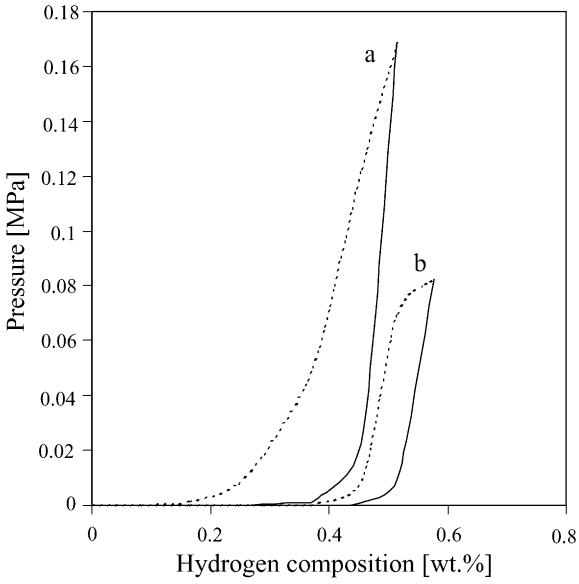

Fig. 4. Electrochemical isotherms pressure-composition for absorption (dashed line) and desorption (solid line) of hydrogen on TiNi alloys: (a) amorphous, (b) nanocrystalline.

Table 1 reports the discharge capacities of the studied nanocrystalline TiNi-type materials. The discharge capacity of the electrodes prepared by application of MA TiNi alloy powder is low (Fig. 5). Materials obtained by the substitution of Ni for Zr in $TiNi_{1-x}Zr_x$ lead to great improvement in activation behaviour of the electrodes. In the annealed nanocrystalline $TiNi_{0.875}Zr_{0.125}$ powder, discharge capacity of up to 135 mA h g^{-1} was measured. The electrodes mechanically alloyed and annealed from the elemental powders displayed maximum capacities at around the third cycle, but especially for $TiNi_{0.75}Fe_{0.125}Zr_{0.125}$ alloy, degraded slightly with cycling. This may be due to the easy formation of an oxide layer (TiO_2) during the cycling.

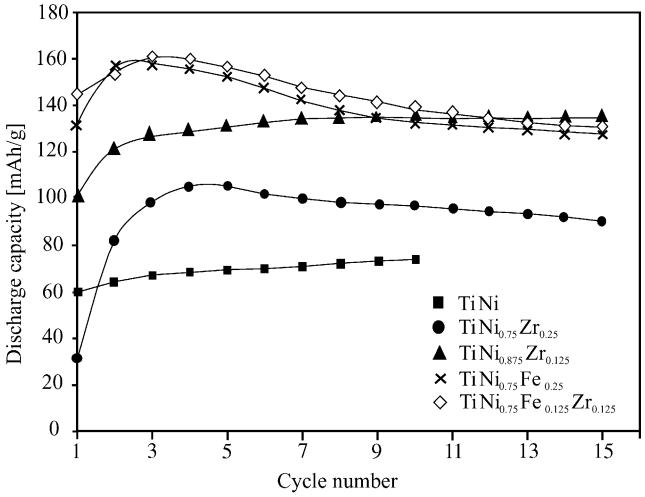

Fig. 5. Discharge capacity as a function of cycle number of electrode prepared with TiNi-type alloys (discharge current 40 mA g^{-1}, 6 M KOH, T = 20 °C).

On the other hand, the discharge capacity of nanocrystalline $TiNi_{0.875}Zr_{0.125}$ powder has not changed much during cycling (Fig. 5). The alloying elements Zr, substituted simultaneously for nickel atoms in nanocrystalline $TiNi_{1-x}M_x$ master alloy, prevented oxidation of this electrode material. Additionally, it was found that the substitution of nickel by Zr in $TiFe_{0.125}M_{0.125}Ni_{0.75}$ materials leads to an increase in discharge capacity in comparison to basic alloy. In these annealed nanocrystalline powders, discharge capacities up to 158 mA h g^{-1} were measured (Fig. 5).

Application of titanium alloys as hydrogen storage materials focused our attention also on the electronic structure of TiNi and its modification by Zr and Fe atoms [17]. The significant broadening of the valence band for the nanocrystalline TiNi-based alloys could be explained by a strong deformation of the nanocrystals. Normally, the interior of the nanocrystal is contracted and the distances between atoms located at the grain boundaries are expanded [18]. Furthermore, in the case of MA nanocrystalline $TiNi_{0.75}Fe_{0.25}$, $TiNi_{0.875}Zr_{0.125}$ and $TiNi_{0.75}Fe_{0.125}Zr_{0.125}$ alloys, the Ni atoms could also occupy metastable positions in the deformed grain. The above behaviour can also modify the electronic structure of the valence band. As a result, the strong modifications of the electronic structure of the nanocrystalline TiNi-type alloys compared to that of polycrystalline materials could significantly influence their hydrogenation properties.

4. Conclusion

In conclusion, nanocrystalline TiNi-based alloys synthesized by MA and annealing were used as negative electrode materials for Ni-MH_x battery. The discharge capacities of electrodes prepared by application of MA and annealed TiNi alloy powders displayed low capacities. It was found that the respective replacement of Ni in TiNi by Zr or Zr and Fe improved not only the discharge capacity but also the cycle life of these electrodes.

Acknowledgements

This project was supported by the Polish National Committee for Scientific Research (KBN). The glove box Labmaster 130 (M. Braun) was purchased by the Foundation for Polish Science under the program TECHNO-2000.

References

[1] A. Anani, A. Visintin, K. Petrov, S. Srinivasan, J.J. Reilly, J.R. Johnson, R.B. Schwarz, P.B. Desch, J. Power Sources 47 (1994) 261.
[2] L. Zaluski, A. Zaluska, J.O. Ström-Olsen, J. Alloys Comp. 253–254 (1997) 70.
[3] M. Jurczyk, Curr. Top. Electrochem. 9 (2003) 105.
[4] M. Jurczyk, E. Jankowska, M. Nowak, J. Jakubowicz, J. Alloys Comp. 336 (2002) 265.

[5] G. Liang, J. Huot, R. Schulz, J. Alloys Comp. 320 (2001) 133.
[6] M. Jurczyk, Bull. Pol. Ac.: Tech. 52 (2004) 67.
[7] J.S. Benjamin, Sci. Am. 234 (1976) 40.
[8] C. Suryanarayna, Progr. Mater. Sci. 46 (2001) 1.
[9] J.J. Reilly, Z. Phys. Chem. 117 (1979) 155.
[10] R. Burch, N.B. Mason, J. Chem. Soc. Faraday Trans. I 75 (1979) 561.
[11] M.H. Mintz, S. Vaknin, S. Biderman, Z. Hadari, J. Appl. Phys. 52 (1981) 463.
[12] K. Oguro, Y. Osumi, H. Suzuki, A. Kato, Y. Imamura, H. Tanaka, J. Less-Common Met. 89 (1983) 275.
[13] C.S. Wang, Y.Q. Lei, Q.D. Wang, J. Power Sources 70 (1998) 222.
[14] S. Wakao, Y. Yonemura, J. Less-Common Met. 89 (1983) 481.
[15] D.Y. Song, X.P. Gao, Y.S. Zhang, D.F. Lin, Z.X. Zhou, G.S. Wang, P.W. Shen, J. Alloys Comp. 199 (1993) 161.
[16] M. Jurczyk, E. Jankowska, M. Makowiecka, I. Wieczorek, J. Alloys Comp. 354 (2003) L1.
[17] M. Jurczyk, L. Smardz, A. Szajek, Mat. Sci. Eng. B 108 (2004) 67.
[18] M.R. Fitzsimmons, J.A. Estman, R.A. Robinson, A.C. Lawson, J.D. Thompson, R. Morshovich, Phys. Rev. B 48 (1993) 8245.